



Desorption due to recoil induced by neutrino emission and Auger relaxation of  $^{37}\text{Cl}$  following the electron capture decay of  $^{37}\text{Ar}$   
by Lin Zhu

A thesis submitted in partial fulfillment of the requirements for the degree of Doctor of Philosophy in Physics  
Montana State University  
© Copyright by Lin Zhu (1995)

Abstract:

A novel experiment was developed in this work to study the desorption and the Auger relaxation processes of  $^{37}\text{Cl}$  following the  $^{37}\text{Ar}$  electron capture decay. For the first time, the desorption of  $^{37}\text{Cl}$  ions due to recoil induced by neutrino emission in this decay process was observed. The kinetic energy distribution of the desorbing  $^{37}\text{Cl}$  ions was accurately measured by using coincidence techniques. The resulting  $^{37}\text{Cl}$  ion energy ranges from 5 eV to 13 eV with a maximum at around 9 eV and an FWHM about 3 eV. The charge state distribution of the desorbing  $^{37}\text{Cl}$  ions was also measured. The resulting charge state distribution is: 53% of the total ions have charge  $+e$ , 21% have charge  $+2e$  and 26% have charge  $+ne$ , where  $n \geq 3$ . The desorbing probability of  $^{37}\text{Cl}$  ions was measured by two independent experiments which gave the result of  $9.4 \pm 1.2\%$ . The energy distribution, the charge state distribution and the desorbing probability of  $^{37}\text{Cl}$  ions are all quite different as compared with the expected values for an isolated Cl atom. These differences are explained in the desorption model involving charge exchange and Coulomb repulsion between  $^{37}\text{Cl}$  ions and their surrounding atoms.

The electron capture decay also creates a highly unusual initial state in the  $^{37}\text{Cl}$  atom which allows direct observation of some novel relaxation processes which are amenable to many body theory, but essentially impossible to probe experimentally with conventional techniques. For the first time, direct evidence of the double Auger decay of a K-hole and the large shift in energy (22 eV) of an LMM Auger line was reported. The double Auger decay probability and energy distribution of the two double Auger electrons were measured by using coincidence techniques. The resulting double Auger decay probability ranges from  $12 \pm 0.3\%$  to  $15 \pm 0.4\%$  of the total Auger decay. The preferred energy distribution of the double Auger emission is for one of the electrons to take most of the energy, with the second receiving the small remaining balance. A model explaining the large shift in energy of an LMM Auger line is also provided.

DESORPTION DUE TO RECOIL INDUCED BY NEUTRINO EMISSION  
AND AUGER RELAXATION OF  $^{37}\text{Cl}$  FOLLOWING  
THE ELECTRON CAPTURE DECAY OF  $^{37}\text{Ar}$

by

LIN ZHU

A thesis submitted in partial fulfillment  
of the requirements for the degree

of

Doctor of Philosophy

in

Physics

MONTANA STATE UNIVERSITY—BOZEMAN  
Bozeman, Montana

May 1995

D378  
Z609

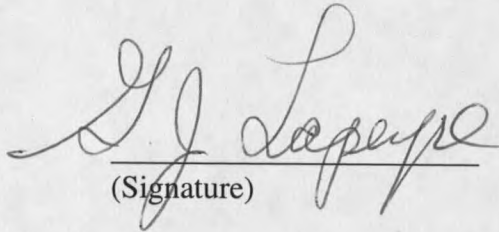
APPROVAL

of a thesis submitted by

LIN ZHU

This thesis has been read by each member of the thesis committee and has been found to be satisfactory regarding content, English usage, format, citations, bibliographic style, and consistency, and is ready for submission to the College of Graduate Studies.

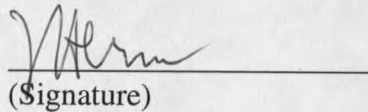
Dr. Gerald Lapeyre

  
\_\_\_\_\_  
(Signature)

6-9-95  
(Date)

Approved for the Department of Physics

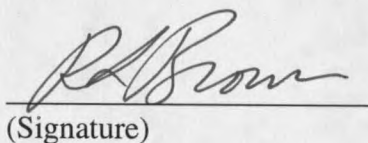
Dr. John Hermanson

  
\_\_\_\_\_  
(Signature)

6-9-95  
(Date)

Approved for the College of Graduate Studies

Dr. Robert Brown

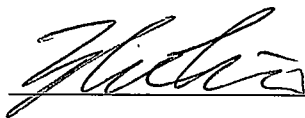
  
\_\_\_\_\_  
(Signature)

6/29/95  
(Date)

## STATEMENT OF PERMISSION TO USE

In presenting this thesis in partial fulfillment of the requirements for a doctoral degree at Montana State University—Bozeman, I agree that the Library shall make it available to borrowers under the rules of the Library. I further agree that copying of this thesis is allowable only for scholarly purposes, consistent with "fair use" as prescribed in the U.S. Copyright Law. Requests for extensive copying or reproduction of this thesis should be referred to University Microfilms International, 300 North Zeeb Road, Ann Arbor, Michigan 48106, to whom I have granted "the exclusive right to reproduce and distribute my dissertation in and from microform along with the non-exclusive right to reproduce and distribute my abstract in any format in whole or part."

Signature

A handwritten signature in cursive script, appearing to read "Richard", written over a horizontal line.

Date

6-9-95

DEDICATED TO MY GRANDMOTHER  
AND MY PARENTS

## VITA

Lin Zhu was born on October 29, 1962 in Beijing, China to Shijun Zhu and Wenjuan Xiang. He has a younger sister, Hong Zhu.

Lin Zhu was raised in the beautiful campus of Tsinghua University, Beijing China where he attended the university-attached primary school in 1969, junior high school in 1974 and high school in 1977. In 1980, he was admitted to Tsinghua University, one of the best schools in China. He completed his undergraduate education with a B.S. degree in electrical engineering in 1985. In the same year, he started his graduate study in the Graduate College of Tsinghua University. From 1987 to 1989, he studied in the Physics Department of the Technical University of Munich, Munich, West Germany. In 1989, he came to the wonderful small town called Bozeman. He got his M.S. degree in physics from Montana State University in 1992.

## PREFACE

Eight years ago, when Dr. Avci, a surface scientist met Dr. Hindi, a nuclear physicist half a world away in Saudi Arabia, they came up with a brilliant idea: using surface analysis techniques to study nuclear reactions. Six years ago, Dr. Menzel invited me to his office, "I just talked to Prof. Lapeyre in Montana. You should not disappoint them when you get there," he told me in German, "because I have just put up a lot of good words for you." Four years ago, there began this research project. With the help of a German professor, I got the opportunity to work under the guidance of professors with Turkish, Lebanese and American origin. I would like to dedicate this report to these mentors who have shown me how small this world could be for physicists.

My sincere thanks to those who made this possible. To Dr. Lapeyre for his help in my coming to this great country, for his continuous support, supervision and confidence in me. To Dr. Avci for his scientific inspiration, encouragement and patient guidance throughout this thesis work. To Dr. Hindi who has helped me throughout this project with his sharp instincts in physics and tireless working spirits. To Dr. Anderson for his important criticisms and advice that have been and will remain as a beneficial experience for me. To Dr. Smith, Dr. Tuthill and Department Chairman, Dr. Hermanson for their great support in my graduate study. To the wonderful staff, Alice, Margaret and Rose for their cheerful help. To Erik and Norm for their excellent technical support.

## TABLE OF CONTENTS

	Page
VITA.....	v
PREFACE.....	vi
TABLE OF CONTENTS.....	vii
LIST OF TABLES.....	x
LIST OF FIGURES.....	xi
ABSTRACT.....	xv
1. INTRODUCTION.....	1
Concepts of the Work.....	2
Desorption due to Recoil Induced by Neutrino Emission.....	2
Surface Interactions of $^{37}\text{Cl}$ Ion.....	5
Auger Relaxation of $^{37}\text{Cl}$ Atom.....	8
Historical Review of Related Works.....	10
2. THEORY.....	14
Recoil Induced by Neutrino Emission.....	14
Models on Stimulated Desorption.....	17
The Menzel-Gomer-Redhead (MGR) Model.....	18



TABLE OF CONTENTS—Continued

	Page
The Knotek-Feibelman (KF) Model.....	22
Desorption Due to "Coulomb Explosion" .....	25
Theory of Auger Transition.....	29
Auger Effect.....	29
Auger Energies and Intensities.....	33
Double Auger Transition.....	38
3. EXPERIMENT.....	45
Experimental Setups.....	45
The UHV System.....	46
The Substrates.....	49
The Detectors.....	51
The Position Sensitive Detector.....	56
The Radioactive $^{37}\text{Ar}$ Sources.....	61
Coincidence Techniques and Electronic Systems.....	66
Experimental Procedure.....	73
4. RESULTS AND DISCUSSIONS.....	77
Desorption due to Recoil Induced by Neutrino Emission.....	77
Energy Distribution of $^{37}\text{Cl}$ Ions.....	77
Charge-State Distribution of $^{37}\text{Cl}$ Ions.....	83

TABLE OF CONTENTS—Continued

	Page
Results on Multiple and Mixed Layers.....	91
Desorption Probability of $^{37}\text{Cl}$ Ions.....	95
Discussion of the Desorption Results.....	99
Auger Relaxation of a $^{37}\text{Cl}$ atom.....	108
$^{37}\text{Cl}$ LLM and LMM Auger Peaks.....	109
Discussion of $^{37}\text{Cl}$ LMM Auger Results.....	113
Double Auger Decay of a $^{37}\text{Cl}$ atom.....	117
$^{37}\text{Cl}$ Double Auger Probability.....	118
$^{37}\text{Cl}$ Double Auger Energy Distribution.....	127
Discussion of $^{37}\text{Cl}$ Double Auger Decay Results.....	133
5. CONCLUSIONS.....	140
Conclusions.....	140
Perspective on Neutrino Mass Limit Study.....	143
REFERENCES.....	146
APPENDICES.....	156
Appendix A: Introduction to Neutrino Physics and Neutrino Mass Limit Study.....	156
Appendix B: Designing Diagrams of the Detectors.....	168
Appendix C: Plasmon Decay into Multi-Electron-Hole Pairs in Si(111)...	176

## LIST OF TABLES

Table	Page
2.1 Table of the Energies, Symbols and Number of Electrons for Ar and Cl Core Levels.....	29
2.2 Table of Final States of Ar KLL Auger Series.....	32
2.3 Table of Ar LMM Auger Energies and Relative Intensities.....	36
2.4(a) Table of Auger Transition Probabilities for a K-hole Vacancy.....	36
2.4(b) Table of Auger Transition Probabilities for L-hole Vacancies.....	37
2.5 Table of Final Charge State Distribution of Ar after Auger Transition of an 1s Initial Hole.....	38
4.1 Table of Charge State Distribution Results from Experiments and Simulations.....	84
A1.1 Table of the Three Generations of Quarks and Leptons.....	161
A1.2 Table of Neutrino Mass Fitting Results.....	165

## LIST OF FIGURES

Figure	Page
1.1 Electron capture decay and $^{37}\text{Cl}$ ions desorption in $^{37}\text{Ar} \rightarrow ^{37}\text{Cl} + \nu$ .....	3
1.2 The original 9.5 eV recoil energy and the additional energy due to charge exchange and Coulomb repulsion of the $^{37}\text{Cl}$ ions.....	6
1.3 The unusual initial state of $^{37}\text{Cl}$ atom from EC decay.....	9
1.4 Normal Auger transition and double Auger transition.....	10
2.1 The energy level scheme of MGR model.....	19
2.2 The energy level scheme of Antoniewicz model.....	21
2.3 The KF model for $\text{O}^+$ ion desorption.....	23
2.4 Schematic displaying terms of a Hubbard Hamiltonian with intrasite Coulomb term $U_{\text{eff}}$ .....	27
2.5 KLL Auger transition and LLM Coster-Koing Auger transition.....	30
2.6 Energy changes of an Auger electron entering analyzer with work function.....	34
2.7 Relative intensities of Auger peaks of Ar with 1s hole calculated by using RACS.....	37
2.8 Brueckner-Goldstone diagrams for the partial amplitudes of double Auger decay.....	40
2.9 Diagrams for double Auger decay models.....	42
2.10 Double Auger energy distribution calculated for atomic Ne.....	43
3.1 UHV system schematics.....	47

LIST OF FIGURES—Continued

Figure	Page
3.2 Auger peaks of Ar and Carbon from the substrates at different temperatures.....	48
3.3 TPD spectrum of Ar from the graphite substrate.....	50
3.4 The mounting bridge between the graphite substrate and the cold finger.....	51
3.5 Diagram of the home-made channeltron based detector.....	53
3.6 Diagram of the home-made microchannel plates based detector.....	55
3.7 MCP pulse high distribution and detecting efficiencies for electron and ion.....	55
3.8 Geometry of a circular arc terminated resistive anode encoder.....	59
3.9 Diagram of the home-made MCP-RAE based PSD detector.....	60
3.10 The gamma ray spectrum of the radioactive gas source taken by an HP-Ge detector.....	62
3.11 The gamma ray spectrum of the $^{37}\text{Ar}$ gas source.....	63
3.12 Double sealing $^{40}\text{Ca}$ in quartz ampoules before nuclear irradiation.....	65
3.13 Schematic diagram of the first coincidence measurement system.....	67
3.14 True coincidence counts and accidental coincidence counts.....	68
3.15 Schematic diagram of the second coincidence measurement system.....	70
3.16 The logic block diagram of the second coincidence measurement system.....	71
4.1 The Monte-Carlo simulation of the $^{37}\text{Cl}$ ion recoil velocity distribution.....	79

LIST OF FIGURES—Continued

Figure	Page
4.2 Time-of-flight spectrum obtained by using coincidence measurement and the corresponding energy spectrum of the desorbing $^{37}\text{Cl}$ ion.....	81
4.3 Comparison of ToF spectra between the Monte-Carlo simulations and the experimental results.....	82
4.4 Using retarding field energy analyzer to measure charge state distribution.....	85
4.5 Retarding field energy spectrum of the desorbing $^{37}\text{Cl}$ ion.....	86
4.6 Calculating charge state distribution from the RFE spectrum.....	87
4.7 Comparison of charge state distribution and the REF spectra between the Monte-Carlo simulation and the experimental results.....	89
4.8 Comparison of the maximum kinetic energy obtained by ToF and RFE spectra.....	90
4.9 RFE spectra of desorbing $^{37}\text{Cl}$ ion at different coverage.....	92
4.10 Comparison of RFE spectra, total ion counts and maximum kinetic energies among different mixtures of radioactive and stable Ar.....	93
4.11 Comparison of energy distribution of desorbing $^{37}\text{Cl}$ ion from different coverage.....	95
4.12 KLL and LMM Auger electron-electron coincidence ToF spectrum.....	98
4.13 Local environment of $^{37}\text{Cl}$ ion.....	100
4.14 The simulation results of $\text{Cl}^+$ ion exchange charge with metal surface.....	104
4.15 The model explaining charge exchange and Coulomb repulsion during $^{37}\text{Cl}$ ion desorption.....	106
4.16 The RAE spectrum of $^{37}\text{Cl}$ LMM Auger.....	110

LIST OF FIGURES—Continued

Figure	Page
4.17 Comparison of LMM Auger spectra among $^{37}\text{Cl}$ following EC decay, Cl from CsCl and physisorbed $^{40}\text{Ar}$ .....	111
4.18 $^{37}\text{Cl}$ LMM Auger spectrum measured with new radioactive source.....	113
4.19 Comparison between $^{37}\text{Cl}$ LMM Auger spectrum and Cl conventional Auger lines.....	114
4.20 The Auger cascade model explaining the LMM <sup>H</sup> peak.....	116
4.21 Spectrum of coincidence measurement between KLL Auger and LMM Auger.....	119
4.22 Spectrum of coincidence measurement between two Double Auger electrons.....	120
4.23 The RFE spectrum of $^{37}\text{Cl}$ LMM Auger by the MCP detector.....	123
4.24 Spectra of coincidence measurement for KLL and LMM Auger electrons with different retarding screen voltages.....	126
4.25 Spectra of coincidence measurement for double Auger electrons with different retarding screen voltages.....	128
4.26 Double Auger energy distribution.....	130
4.27 Differential energy dependence of the double Auger probability as compared with theoretical prediction.....	131
4.28 Double Auger energy distribution measured with the new source.....	132
4.29 Schematic diagram of a triple coincidence spectrum.....	134
4.30 Comparison of double Auger coincidence spectra between experimental and simulation results.....	138

## ABSTRACT

A novel experiment was developed in this work to study the desorption and the Auger relaxation processes of  $^{37}\text{Cl}$  following the  $^{37}\text{Ar}$  electron capture decay. For the first time, the desorption of  $^{37}\text{Cl}$  ions due to recoil induced by neutrino emission in this decay process was observed. The kinetic energy distribution of the desorbing  $^{37}\text{Cl}$  ions was accurately measured by using coincidence techniques. The resulting  $^{37}\text{Cl}$  ion energy ranges from 5 eV to 13 eV with a maximum at around 9 eV and an FWHM about 3 eV. The charge state distribution of the desorbing  $^{37}\text{Cl}$  ions was also measured. The resulting charge state distribution is: 53% of the total ions have charge  $+e$ , 21% have charge  $+2e$  and 26% have charge  $+ne$ , where  $n \geq 3$ . The desorbing probability of  $^{37}\text{Cl}$  ions was measured by two independent experiments which gave the result of  $9.4 \pm 1.2\%$ . The energy distribution, the charge state distribution and the desorbing probability of  $^{37}\text{Cl}$  ions are all quite different as compared with the expected values for an isolated Cl atom. These differences are explained in the desorption model involving charge exchange and Coulomb repulsion between  $^{37}\text{Cl}$  ions and their surrounding atoms.

The electron capture decay also creates a highly unusual initial state in the  $^{37}\text{Cl}$  atom which allows direct observation of some novel relaxation processes which are amenable to many body theory, but essentially impossible to probe experimentally with conventional techniques. For the first time, *direct* evidence of the double Auger decay of a K-hole and the large shift in energy (22 eV) of an LMM Auger line was reported. The double Auger decay probability and energy distribution of the two double Auger electrons were measured by using coincidence techniques. The resulting double Auger decay probability ranges from  $12 \pm 0.3\%$  to  $15 \pm 0.4\%$  of the total Auger decay. The preferred energy distribution of the double Auger emission is for one of the electrons to take most of the energy, with the second receiving the small remaining balance. A model explaining the large shift in energy of an LMM Auger line is also provided.



## CHAPTER 1

## INTRODUCTION

On February 23, 1987, a supernova burst in the Large Magellanic Cloud (SN1987a) and sent rays of neutrinos to the earth. The sudden release of the  $10^{53}$  erg of energy from the dying star triggered merely 100 or so “neutrino” counts in huge underground detectors around the world. This, however, caused enough excitement for several groups of physicists—the burst of SN1987a gave them a golden opportunity to study the mysteries of neutrinos.<sup>1,2</sup> Among these mysteries, the biggest one is whether neutrino has a rest mass or not, and what that mass might be. The neutrino mass problem is one of the most fundamental questions in physics. The answer to this question could have profound implications for particle physics, astrophysics and cosmology.<sup>3</sup>

The mass information of a neutrino can be obtained from a nuclear reaction involving the creation or annihilation of a neutrino.<sup>1-3</sup> One of these kinds of nuclear reactions is the electron capture (EC) decay. In this thesis, the desorption due to recoil induced by neutrino emission and the Auger relaxation processes of  $^{37}\text{Cl}$  following the EC decay of  $^{37}\text{Ar}$  is reported. It is demonstrated in this work that the EC decay of  $^{37}\text{Ar}$  provides not only a possible approach to the neutrino mass problem but also a rare

opportunity for some novel studies in surface and atomic physics.<sup>4-7</sup> The focal point of this thesis is to report the results of these novel studies.

The problems addressed in this thesis work fall into two categories: The first one is the study of the desorption due to recoil induced by neutrino emission in the EC decay process,  $^{37}\text{Ar} \rightarrow ^{37}\text{Cl} + \nu$ , where  $\nu$  is a neutrino. In this EC decay process, could the emission of the neutrino cause enough recoil of the adsorbed daughter atom  $^{37}\text{Cl}$  to break the absorption bond? If the desorption does occur, what factors would affect the energy distribution of those desorbing daughter atoms? The second category is the study of the Auger relaxation processes of the  $^{37}\text{Cl}$  daughter atom. The EC decay creates a deep vacancy in the energy levels of the  $^{37}\text{Cl}$  atom while the whole atom is still in a neutral charge state. As discussed later, this initial state is highly unusual as compared with those commonly encountered initial excitations. What are the relaxation processes or the decay channels associated with this particular initial state? To better understand these questions, the concepts of these studies will be introduced first in the following paragraphs.

### Concepts of the Work

#### Desorption due to Recoil Induced by Neutrino Emission

The first part of the study is to measure the spectrum of recoil velocities of  $^{37}\text{Cl}$  ions following the EC decay of  $^{37}\text{Ar}$  physisorbed on a well defined surface. In this EC

decay process which converts  $^{37}\text{Ar}$  into  $^{37}\text{Cl}$ , a proton in the nuclei of  $^{37}\text{Ar}$  captures a 1s or 2s electron and becomes a neutron, while a neutrino is emitted and the  $^{37}\text{Cl}$  daughter atom recoils in the direction opposite to that in which the neutrino moves. This recoil may break the bond between the  $^{37}\text{Cl}$  atom and the substrate and cause desorption of the  $^{37}\text{Cl}$  ions from the surface (Fig. 1.1). The initial 1s or 2s vacancy created by the EC process will decay through Auger cascades or x-ray emission. Therefore the daughter  $^{37}\text{Cl}$  atom is usually multiple ionized after the EC decay.

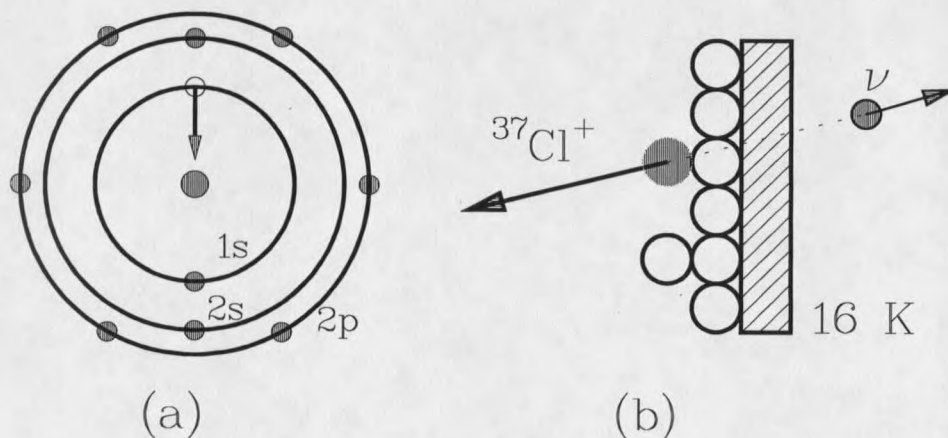


Figure 1.1. (a) Electron is captured from a low (1s) orbital:  $^{37}\text{Ar} \rightarrow ^{37}\text{Cl} + \nu$ . (b)  $^{37}\text{Cl}$  ion recoils and desorbs from surface due to neutrino emission.

For an isolated  $^{37}\text{Ar}$  atom, the recoil process is a two-body problem with a total reaction energy,  $Q = 814$  keV (Ref. 8). Energy and momentum conservation dictates that

the recoil energy must be 9.54 eV, if a massless neutrino with about 814 keV of energy is emitted. If a neutrino with mass  $m_\nu$  is also emitted in a certain fraction of the EC decays, then the corresponding recoiling ions will have lower kinetic energy. The fractional change in recoil kinetic energy is  $\Delta E/E = (m_\nu/Q)^2$  (Ref. 3), where  $Q$ , the total reaction energy is the rest mass ( $mc^2$ ) difference between  $^{37}\text{Ar}$  and  $^{37}\text{Cl}$ . Thus the heaviest massive neutrino that could be emitted in this EC decay would have a rest mass of 814 keV. If a 250-keV neutrino were to be emitted, for example, the fractional change in recoil energy of the  $^{37}\text{Cl}$  would be 9.4%. The lowest neutrino mass to which this method could be sensitive depends on the ability to resolve the peak associated with the emission of the massive neutrino from the dominant peak associated with the emission of the massless neutrino in the recoil spectrum.

There are well known and calculable effects that would contribute to the broadening in the recoil energy spectrum for an isolated  $^{37}\text{Ar}$  atom. Some of these effects can be studied by computer simulations. However, for an  $^{37}\text{Ar}$  atom physisorbed on a cold surface, and possibly surrounded by other Ar atoms, it is not obvious whether the recoil due to neutrino emission could break the bond between  $^{37}\text{Cl}$  atom and the substrate and cause desorption. Even if the desorption does occur, it is still much more difficult, as compared to the isolated  $^{37}\text{Ar}$  case, to determine what effects would contribute to the broadening in the recoil energy spectrum. To approach these questions, it is necessary to examine the surface interactions during the  $^{37}\text{Cl}$  ion desorption process.

## Surface Interactions of $^{37}\text{Cl}$ Ion

Adsorption and stimulated desorption have been very useful tools to study surfaces. Since the 1960s, several models have been developed to describe the interactions between adsorbates and the substrates. Current models involve detailed knowledge of surface binding energies, adsorption site symmetries and potentials, substrate phonon spectra, and surface electronic structures.<sup>9-12</sup> The neutrino recoil in this work provides an entirely new way to study the desorption dynamics. A simple model of the desorption in this case is described as follows: First, the adsorbed  $^{37}\text{Ar}$  atoms undergo EC decay and become  $^{37}\text{Cl}$  ions with 9.54 eV recoil energy to move away from the surface. Before these  $^{37}\text{Cl}$  ions can leave the surface, the interactions between the  $^{37}\text{Cl}$  ions and the substrate will result in additional kinetic energies on the top of the 9.54 eV recoil energy. These additional energies will contribute to the broadening of the recoil energy spectrum. One of the major goals in this work is to understand these interactions.

The first interaction to be discussed is the bonding between  $^{37}\text{Ar}$  and the cold substrates. The  $^{37}\text{Ar}$  atom is physisorbed on gold or graphite substrates. At the critical temperature of 65 K Ar begins to form a monolayer on these substrates. By about 30 K, multiple adsorbed layers (Ar ice) are formed.<sup>13-15</sup> It has been found that these multiple adsorbed layers are likely to form a face-centered cubic (fcc) polycrystalline layer at the experimental temperature of 16 K.<sup>16</sup> Therefore the adsorbed Ar could actually form a band structure and solid state physics has to be taken into account. The bonding between

an  $^{37}\text{Ar}$  atom and the substrate or the neighboring Ar atoms is established through the van der Waals interaction which gives rise to a binding energy of about 100 meV.<sup>15</sup> This interaction cannot play a major role in the broadening of the recoil energy spectrum because the 100 meV interaction energy is much less than the 9.54 eV recoil energy.

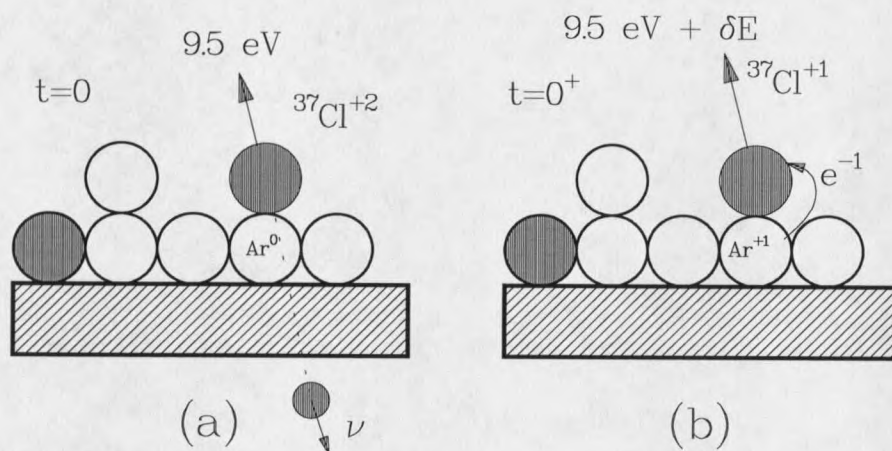


Figure 1.2 (a)  $^{37}\text{Cl}$  ion obtains 9.5 eV recoil energy from neutrino emission. (b) Charge is transferred and Coulomb repulsion gives additional energy  $\delta E$  to the outgoing  $^{37}\text{Cl}$  ion.

The second interaction to be discussed is the charge exchange between the  $^{37}\text{Cl}$  ions and their local surrounding atoms.<sup>17-21</sup> Theoretical calculations and experiments have shown that in the gas phase the EC decay of  $^{37}\text{Ar}$  will give rise to dominantly  $^{37}\text{Cl}^{3+}$ , the positively threefold-charged ions.<sup>22, 23</sup> It is energetically more favorable for the  $^{37}\text{Cl}^{3+}$  ion to pick up an electron from the neighboring particle, such as an Ar atom, during the initial phase of desorption.<sup>24</sup> These charge exchanges, however, could significantly broaden the

recoil energy spectrum. The positively charged  $^{37}\text{Cl}$  ions and their positively charged neighboring atoms will interact via the Coulomb repulsion giving additional contributions to the kinetic energy of the outgoing  $^{37}\text{Cl}$  ions (Fig. 1.2). In some cases, the additional energy due to this "Coulomb explosion"<sup>25</sup> could reach as high as 6 eV. The charge exchange process and Coulomb repulsion are the main causes of the broadening of the  $^{37}\text{Cl}$  recoil energy spectrum.

The charge exchange process can also cause an outgoing  $^{37}\text{Cl}$  ion to lose all of its positive charges and become a neutral atom while desorbing from the surface.<sup>26-28</sup> The experimental setup in this work can only detect charged particles. An estimation of the neutralization cross section and ion desorption yield per electron capture decay will be given from the experimental and computer simulation results.

There are other interactions that affect the energy distribution of the  $^{37}\text{Cl}$  ions desorbing from the substrate. Two examples of them are the thermal vibration of the  $^{37}\text{Ar}$  atoms on the substrate and the recoil of the  $^{37}\text{Cl}$  ions due to Auger electron emission. The physical and chemical characteristics of the substrates can also play an important role in affecting the energy distribution of the  $^{37}\text{Cl}$  ions. Some of these effects will be calculated using computer simulation to compare with the experimental results.

A full treatment of each of the interactions discussed above is beyond the scope of this work, rather, the emphasis is put on the study of the "Coulomb explosion"

phenomenon which is of great significance for the understanding of this particular desorption process. Because this interaction is the dominant factor in the broadening of the recoil energy spectrum, it also becomes a major obstacle to the neutrino mass limit measurements. The broadening of the recoil spectrum reduces the sensitivity of the neutrino mass limit measurements in this experiment. However, through the present studies the major factors which are responsible for the broadening of the recoil spectrum are understood. Future experiments will be designed with reduced charge exchange effects.

#### Auger Relaxation of $^{37}\text{Cl}$ atom

The electron capture decay of the  $^{37}\text{Ar}$  atom creates a highly unusual electronic configuration in the daughter  $^{37}\text{Cl}$  atom which is not encountered in ordinary non-nuclear physical process. Conventional excitations utilizing electron or photon bombardments generally leave the atom in an ionized initial state. However, in the EC decay a proton and an electron become a neutron, hence the total net charge of the atom is unchanged. The daughter  $^{37}\text{Cl}$  atom remains neutral, even though there is a vacancy in its inner shell—the hole resulting from the capture of a electron. As shown in Fig. 1.3, this initial state is unusual in three ways. First, the electronic configuration of the initial state in  $^{37}\text{Cl}$  atom is like Cl in energy but resembles Ar in structure, *i.e.*, each energy level of the  $^{37}\text{Cl}$  atom is relaxed from the Ar level to Cl level within the decay time but all levels except 1s are still fully occupied with electrons, as in the Ar case. Second, this initial state is a neutral



























































































































































































































































































































































































































